Universality in the structural change of expanded liquid alkali metals along the liquid-vapour coexistence curve

1991 J. Phys.: Condens. Matter 3 827

(http://iopscience.iop.org/0953-8984/3/7/007)

J. Phys.: Condens. Matter 3 (1991) 827–836. Printed in the UK

Universality in the structural change of expanded liquid alkali metals along the liquid–vapour coexistence curve

N Matsuda, H Mori, K Hoshino and M Watabe
Faculty of Integrated Arts and Sciences, Hiroshima University, Hiroshima 730, Japan

Received 30 May 1990

Abstract. The structures of expanded liquid alkali metals, Na, K, Rb and Cs, along the liquid–vapour coexistence curve are investigated theoretically by employing the integral equation method in the modified hypernetted-chain (MHNC) approximation and the molecular dynamics (MD) simulation. Excellent agreement is obtained between the MHNC and the MD results, which also agree well with the experimental results. It is shown from these systematic investigations that the characteristic features of the density dependence of the structure along the liquid–vapour coexistence curve observed for expanded liquid Rb (Franz *et al* 1980) and Cs (Winter *et al* 1987) are common features for expanded liquid alkali metals.

1. Introduction

Although the structure of liquid metals near the triple point has been extensively studied experimentally and theoretically and is considered to be well understood, there has been little experimental work on the structural change of liquid metals over a wide range of densities and temperatures. Recently neutron scattering experiments were carried out for liquid Rb (Franz *et al* 1980, Franz 1980) and Cs (Winter *et al* 1987) from their melting points up to their critical points along the liquid–vapour coexistence curve. The interesting characteristic feature found for these expanded liquid metals is that, when liquid metals are expanded along the liquid–vapour coexistence curve and the density decreases, the number of nearest-neighbour atoms decreases without changing the nearest-neighbour distance.

The structural properties of expanded liquid Rb have been studied by perturbation and integral-equation theories (Bratkovsky *et al* 1982, McLaughlin and Young 1984, Kahl and Hafner 1984, Gonzalez *et al* 1990) and by simulations (Mountain 1978, Tanaka 1980) on the basis of the effective pair potential calculated by the pseudopotential theory with various types of pseudopotentials. Very recently, we (Hoshino *et al* 1990a, 1990b, Mori *et al* 1990) have investigated the structure of expanded liquid Cs along the liquid–vapour coexistence curve by the integral equation theory in the modified hypernetted-chain (MHNC) approximation and by the molecular dynamics (MD) simulation, and succeeded in reproducing the characteristic features of the structure of expanded liquid Cs observed by Winter *et al* (1987).

The purpose of this paper is to investigate theoretically whether the characteristic features of the structure of expanded liquid Cs along the liquid–vapour coexistence curve are common features for all alkali metals or not. For this purpose we have

0953-8984/91/070827 + 10 $03.50

Table 1. Pseudopotential parameters in atomic units.

	a	b	R_c
Na	10	2.0	1.90
K	20	1.7	2.55
Rb	21	1.4	2.85
Cs	22	1.2	3.25

investigated systematically the overall trend of the structural change of expanded liquid Na, K and Rb along the liquid–vapour coexistence curve using the MHNC approximation and the MD simulation based on the pair potentials calculated by using the same type of pseudopotentials and the same dielectric function as those used in our calculation of expanded liquid Cs (Hoshino *et al* 1990a, 1990b, Mori *et al* 1990). By combining our previous results for Cs and the present results, we discuss the universality in the structural change of expanded liquid alkali metals.

2. Pseudopotentials and pair potentials

In this paper we employ a new local empty-core pseudopotential proposed recently by Hasegawa *et al* (1990, hereafter referred to as HHWY potential) given, in atomic units, by

$$v(r) = \begin{cases} 0 & \text{for } r < R_c \\ -(Z/r)(1 + a\exp(-br)) & \text{for } r > R_c \end{cases} \tag{1}$$

where Z is the valency and $Z = 1$ for alkali metals. Here a and b are determined so as to fit this form to the electron–ion potential calculated in the local density functional approximation. The values thus obtained are shown in table 1 for Na, K, Rb and Cs. Only R_c is considered as a disposable parameter. A merit of this analytic form is that its Fourier transform also has a simple analytic form as is given below by equation (3). The parameter R_c is determined so as to reproduce theoretically the position of the first peak and the low q behaviour of the observed structure factor near the triple point. The values of R_c thus determined are also shown in table 1. We assume that the pseudopotential parameters do not depend on density or temperature.

The important feature of the HHWY potential is the inclusion of the core-valence exchange-correlation potential, which has a longer tail than the Hartree potential does, as was pointed out by Hoshino and Young (1986) and Hasegawa *et al* (1990). This effect is substantial for heavy alkali metals such as Rb and Cs near the core radii, although it is less important for Na.

Following a standard procedure, we obtain the effective pair potential $\varphi(r)$ by the pseudopotential theory. That is, the $\varphi(r)$ is given by

$$\varphi(r) = \frac{Z^2}{r} + \frac{1}{(2\pi)^3}\int \frac{q^2}{4\pi}\left(\frac{1}{\varepsilon(q)} - 1\right)|v(q)|^2 \exp(i\boldsymbol{q}\cdot\boldsymbol{r})\,d\boldsymbol{q} \tag{2}$$

where $v(q)$ is the Fourier transform of $v(r)$ and calculated analytically from equation (1) to be

$$v(q) = -(4\pi Z/q^2)\cos qr_c\{1 + [aq^2/(q^2 + b^2)]\exp(-bR_c)(1 + \tan qR_c)\}. \tag{3}$$

The dielectric screening function $\varepsilon(q)$ is given by

$$\varepsilon(q) = 1 - (4\pi/q^2)\chi_0(q)/[1 + (4\pi/q^2)G(q)\chi_0(q)] \tag{4}$$

where $\chi_0(q)$ is the Lindhard function and $G(q)$ is the local field correction, for which we use the form proposed by Ichimaru and Utsumi (1981). Note that the effective pair potential depends on the number density of conduction electrons through the density dependence of $\varepsilon(q)$.

3. Methods of calculation

3.1. Modified hypernetted-chain (MHNC) approximation

It has been proved for various liquid systems (Rosenfeld and Ashcroft 1979, Pastore and Kahl 1987, Kahl and Pastore 1988) that the MHNC approximation is a very good approximation in the sense that it produces results which agree very well with computer simulations as well as experimental results. Therefore, we employ this approximation to investigate the structural change of expanded liquid alkali metals over a wide range of densities.

In the integral equation theory, the Ornstein–Zernike relation

$$h(r) = c(r) + n\int c(|\boldsymbol{r} - \boldsymbol{r}'|)h(r')\,\mathrm{d}\boldsymbol{r}' \tag{5}$$

is supplemented by the closure

$$g(r) = \exp(h(r) - c(r) - \beta\varphi(r) + B(r)) \tag{6}$$

where n is the number density, $\beta = 1/k_BT$, $c(r)$ the direct correlation function, $g(r)$ the pair correlation function, $h(r) = g(r) - 1$ the total correlation function and $B(r)$ the bridge function. In the MHNC approximation (Rosenfeld and Ashcroft 1979) the function $B(r)$ is approximated by the one for the hard sphere system $B_{hs}(r)$, which is specified by a single parameter, i.e. a packing fraction $\eta = \pi n\sigma^3/6$, σ being a hard sphere diameter. In the present work we use the Percus–Yevick solution for $B_{hs}(r)$. To solve the MHNC equations, (5) and (6), numerically, we employ the efficient algorithm due to Gillan (1979).

To determine the bridge function parameter η, we have employed the criterion due to Lado *et al* (1983), in which η is chosen so as to minimize the free energy; the condition is given by

$$\int (g(r) - g_{hs}(r))\,\partial B_{hs}(r)/\partial\eta\,\mathrm{d}\boldsymbol{r} = 0 \tag{7}$$

where $g(r)$ is the pair correlation function calculated in the MHNC approximation for the system described by the effective pair potential $\varphi(r)$. Note that we can obtain similar

Table 2. Temperatures T and densities d. Density data are taken from Franz *et al* (1980) for Rb, Winter *et al* (1987) for Cs and Shpil'rain *et al* (1985) for Na and K.

Na	T(K)	380	820	1400	2000
	d(g cm^{-3})	0.9236	0.8203	0.6819	0.5097
K	T(K)	340	720	1400	1800
	d(g cm^{-3})	0.8285	0.7395	0.5724	0.4583
Rb	T(K)	350	900	1400	1700
	d(g cm^{-3})	1.459	1.214	0.97	0.798
Cs	T(K)	323	773	1373	1673
	d(g cm^{-3})	1.83	1.57	1.21	0.96

results by employing the so-called thermodynamic self-consistency condition to determine the bridge function parameter, but the results are less satisfactory quantitatively for expanded liquid Cs (Hoshino *et al* 1990a, 1990b).

3.2. Molecular dynamics simulation

We have performed a standard MD simulation. In our MD simulation we took the total number of atoms $N = 512$ in a cubic cell $L \times L \times L$. The values of L were chosen so as to reproduce the observed density at each temperature in our simulation cell. We have confirmed that the results for $N = 512$ are in excellent agreement with those obtained for $N = 1000$ in some selected cases, and therefore performed our simulation for $N = 512$. The periodic boundary condition is employed and the cut off of the pair potential or the force range is chosen as $L/2$. The initial configuration was constructed by displacing particles randomly from the simple cubic lattice sites. The total numbers of time steps are 2000–4000 steps with a time step $\Delta t = 2.4 \times 10^{-15}$ s and the last 500 configurations are used to obtain the pair correlation functions. The initial velocities of all particles are chosen to be zero and the velocity scaling method is used to attain the corresponding temperature.

4. Results

We present the results of the MHNC and MD calculations for Na, K and Rb as well as those obtained previously for Cs (Hoshino *et al* 1990a,b, Mori *et al* 1990). The temperatures and the densities used in our calculations are shown in table 2. The values for Rb and Cs correspond to those states for which neutron experiments (Franz *et al* 1980, Winter *et al* 1987) were carried out. As for Na and K, the data of the x-ray experiments (Waseda 1980) are available only at lower temperatures.

Since our calculation is performed by employing the effective pair potential obtained by the pseudopotential perturbation theory, based on the nearly-free-electron model, there is a limitation of its validity; our theory is not applicable when the system is close to the critical point, where the metal–non-metal transition is known to occur for expanded liquid alkali metals. The critical temperatures for Rb and Cs, determined

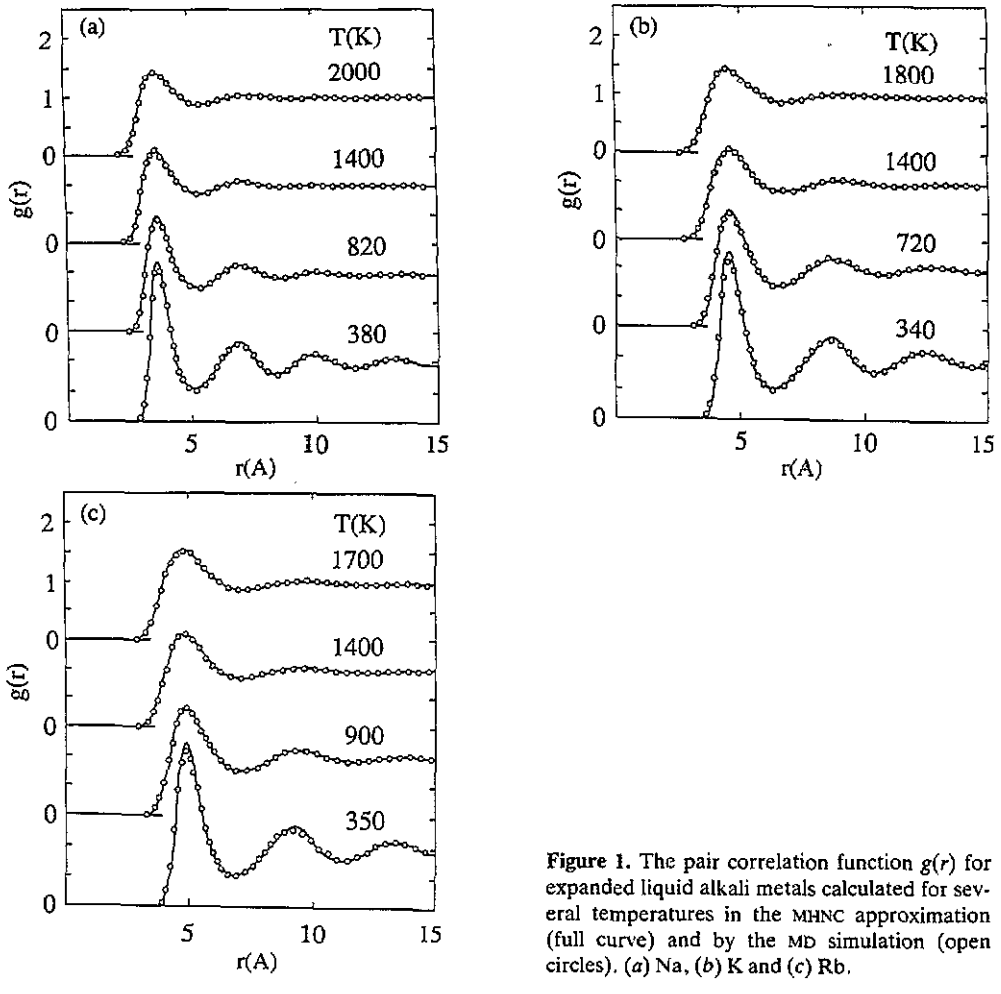

Figure 1. The pair correlation function $g(r)$ for expanded liquid alkali metals calculated for several temperatures in the MHNC approximation (full curve) and by the MD simulation (open circles). (*a*) Na, (*b*) K and (*c*) Rb.

accurately by Jüngst *et al* (1985), are 2017 and 1924 K, respectively, and those for Na and K are estimated to be 2505 and 2280 K, respectively (Shpil'rain *et al* 1985).

4.1. Pair correlation functions

It was shown in our previous paper (Mori *et al* 1990) that the pair correlation functions of expanded liquid Cs calculated in the MHNC approximation are in excellent agreement with those obtained by the MD simulation if we use the same pair potential in both calculations. To see if the MHNC approximation is successful for other alkali metals, we compare the pair correlation functions $g(r)$ for expanded liquid Na, K and Rb calculated in the MHNC approximation with those obtained by the MD simulation in figures 1(*a*), 1(*b*) and 1(*c*), respectively. The agreement between the MHNC and the MD results is excellent in all cases. Since we have used the pair potentials described in section 2 in these calculations, we can confirm the accuracy of the MHNC approximation for expanded liquid alkali metals.

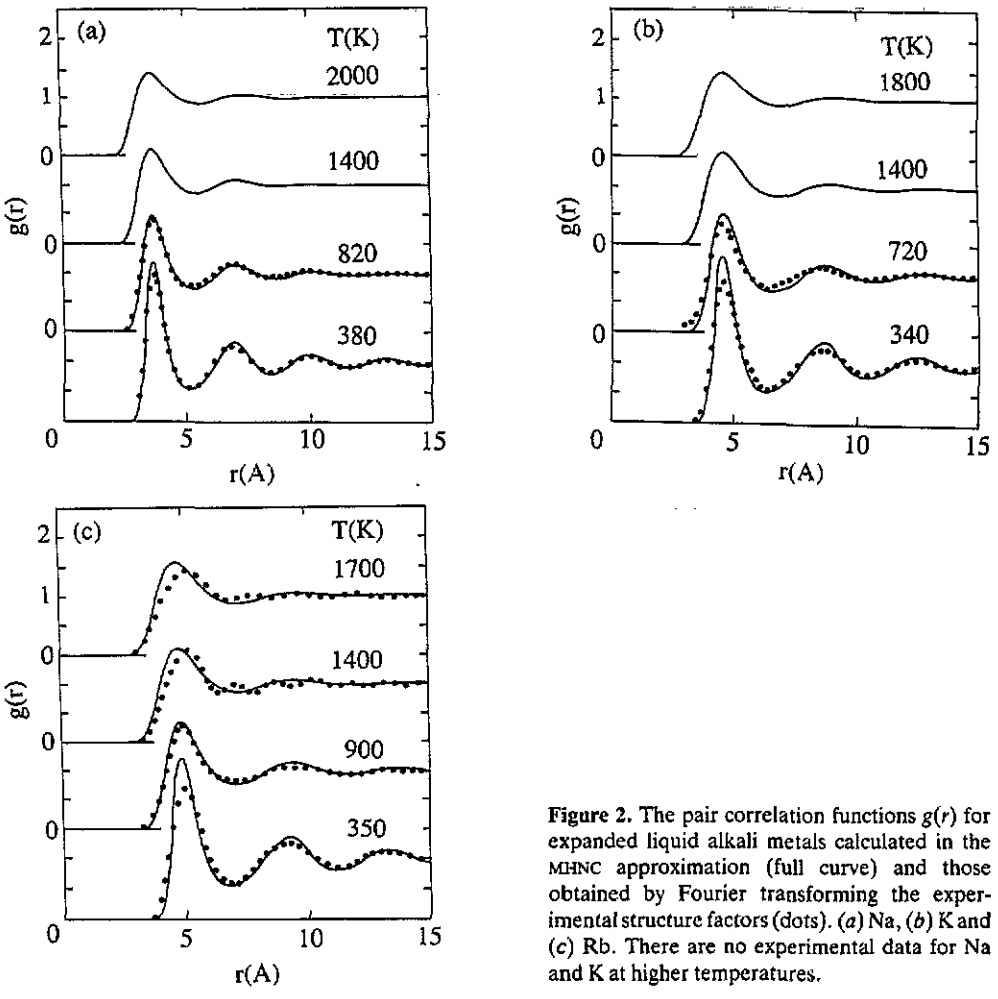

Figure 2. The pair correlation functions $g(r)$ for expanded liquid alkali metals calculated in the MHNC approximation (full curve) and those obtained by Fourier transforming the experimental structure factors (dots). (*a*) Na, (*b*) K and (*c*) Rb. There are no experimental data for Na and K at higher temperatures.

In figures 2(*a*), 2(*b*) and 2(*c*) we compare the pair correlation functions $g(r)$ for expanded liquid Na, K and Rb, respectively, calculated by the MHNC approximation with the 'experimental' ones obtained by Fourier transforming the observed structure factors (Waseda 1980, Franz *et al* 1980). Note that the experimental structure factors for liquid Na and K are available only near the triple point at present, though neutron scattering measurement was carried out for liquid Rb from the triple point to its critical point. It is seen from these figures that the agreement between the theoretical and the experimental results is fairly good when considering the ambiguity due to the numerical Fourier transform of the experimental data, which is available only for a finite range of wave numbers.

One of the most interesting characteristic features of the observed density dependence of the structure of expanded liquid Rb and Cs is the position of the first peak of $g(r)$ that does not change when the density is decreased along the liquid–vapour coexistence curve. To see this feature systematically, we show in figure 3 the positions of the first peaks of $g(r)$ of expanded liquid Na, K, Rb and Cs as a function of density

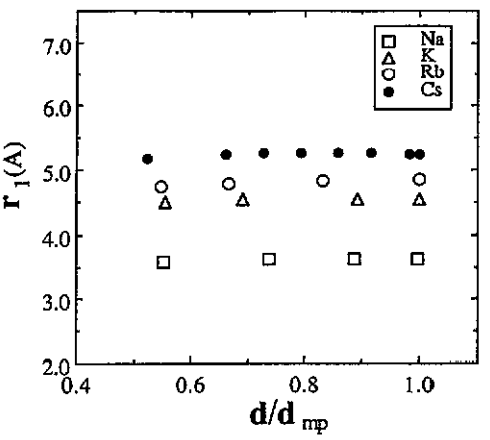

Figure 3. The positions of the first peaks of the pair correlation functions $g(r)$, calculated in the MHNC approximation, of expanded liquid Na, K, Rb and Cs as a function of density d scaled with d_{mp}, the density at the melting temperature.

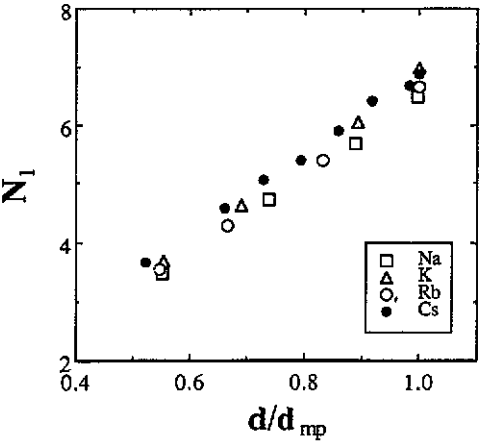

Figure 4. The density dependence of the number of nearest-neighbour atoms, calculated in the MHNC approximation, for expanded liquid Na, K, Rb and Cs.

scaled with the density at the melting temperature. Our theoretical results show that the fact that the positions of the first peak of $g(r)$ do not change along the liquid–vapour coexistence curve is common to all liquid alkali metals.

4.2. Number of nearest neighbour atoms

We have calculated the number of nearest-neighbour atoms N_1, following Winter *et al* (1987), by

$$N_1 = 2n \int_0^{r_1} g(r) 4\pi r^2 \, dr \tag{8}$$

where r_1 is the position of the first peak of $g(r)$. The density dependences of N_1 for expanded liquid Na, K, Rb and Cs are shown in figure 4, where N_1 of each metal is shown as a function of density scaled with its density at the melting point. As is clearly seen from this figure, it is a common feature of expanded liquid alkali metals that the number of nearest-neighbour atoms N_1 decreases almost linearly with respect to density. This feature is consistent with the observed one for expanded liquid Rb (Franz *et al* 1980) and Cs (Winter *et al* 1987), although no data are available for expanded liquid Na and K at present.

4.3. Structure factors

Another interesting structural feature of expanded liquid metals is the density dependence of the structure factor, in particular that of the low q behaviour of $S(q)$. In figures

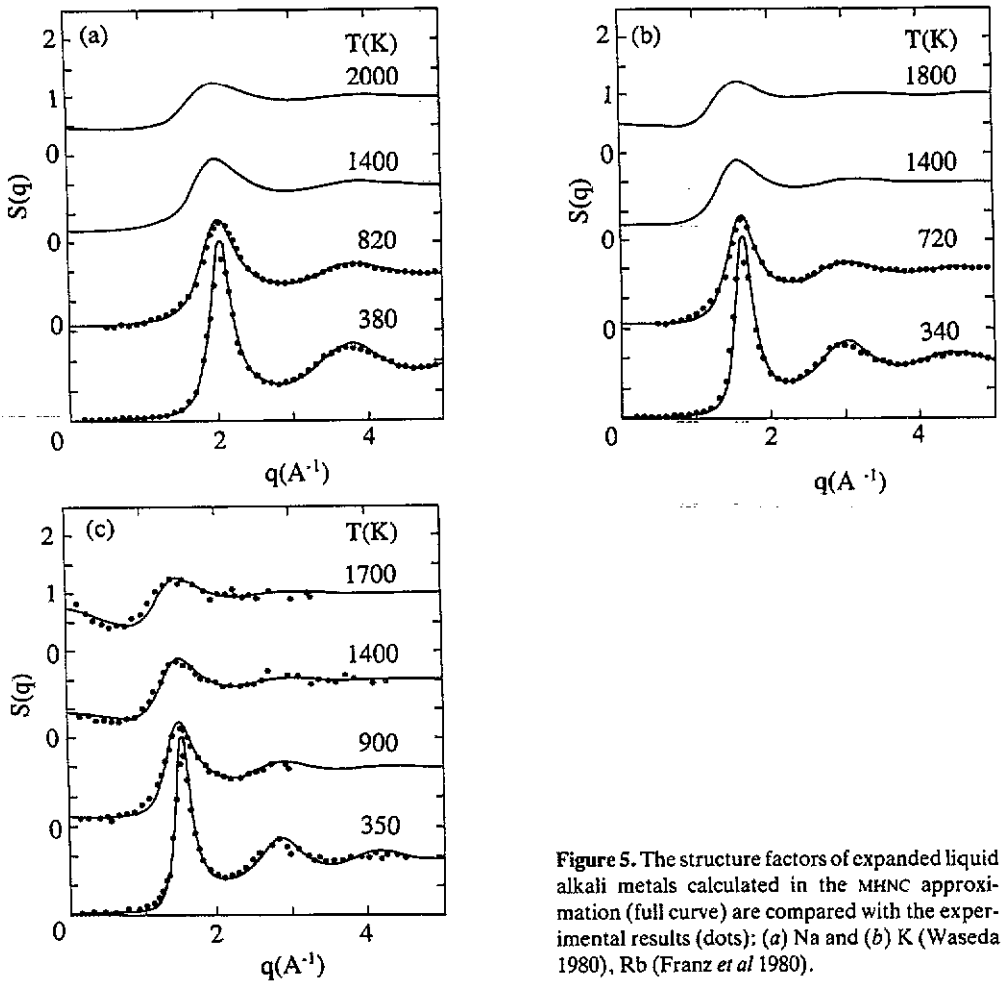

Figure 5. The structure factors of expanded liquid alkali metals calculated in the MHNC approximation (full curve) are compared with the experimental results (dots): (*a*) Na and (*b*) K (Waseda 1980), Rb (Franz *et al* 1980).

5(*a*), 5(*b*) and 5(*c*) we compare the structure factors of Na, K and Rb, respectively, calculated for several temperatures in the MHNC approximation, with experimental results: neutron diffraction results for Rb due to Franz *et al* (1980) and x-ray diffraction results for Na and K due to Waseda (1980), the latter results being available only near the triple points. The agreement between theory and experiment is very good. In the case of Rb, we can reproduce well the density dependence of the $S(q)$ for a wide range of temperatures and densities.

In figure 6 we show the temperature dependence of the heights of the first peaks of $S(q)$ for expanded liquid Na, K, Rb and Cs, where the peak height and the temperature are scaled with their values at the melting point. It is interesting to note that those four kinds of data are well fitted by a single universal curve. Such a feature was also found experimentally by Winter *et al* (1987).

It is interesting to see the increase of the long-wavelength density fluctuation $S(0)$ as the density decreases along the liquid–vapour coexistence curve. We show the theoretical and the experimental $S(0)$ for expanded liquid Na, K, Rb and Cs in figures 7(*a*)

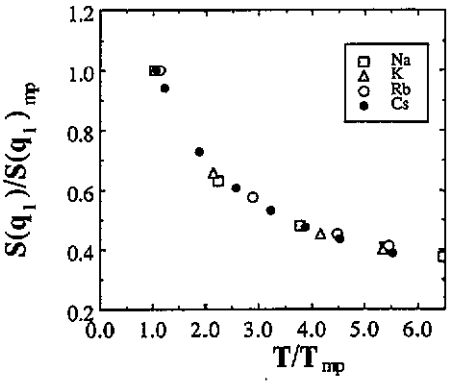

Figure 6. The temperature dependence of the heights of the first peaks of the structure factors, calculated in the MHNC approximation, of expanded liquid alkali metals.

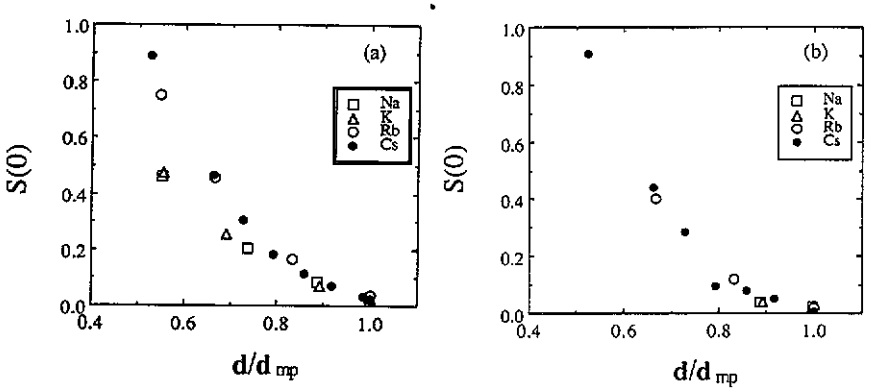

Figure 7. The long-wavelength limit $S(0)$ of the structure factors of expanded liquid alkali metals. (*a*) theory (MHNC), (*b*) experiment.

and 7(*b*), respectively, as a function of density scaled with the density at the melting point. The agreement between theory and experiment is very good, although the experimental data for Na and K are available only near the melting temperature.

5. Summary and discussions

In this paper we have presented the results for the pair correlation functions, the number of nearest-neighbour atoms and the structure factors of expanded liquid alkali metals, Na, K, Rb and Cs, along the liquid–vapour coexistence curve, calculated in the MHNC approximation and by the MD simulation based on the effective pair potentials obtained by the pseudopotential theory. The agreement between the MHNC and the MD results is excellent. These theoretical results also agree well with the experimental results. From these systematic investigations we have found that the characteristic features of the density dependence of the structure along the liquid–vapour coexistence curve observed

for expanded liquid Rb (Franz *et al* 1980) and Cs (Winter *et al* 1987) are common features of expanded liquid alkali metals.

In general, it is important for alkali metals except for Na to take into account the non-locality of the pseudopotential in order to obtain better quantitative agreement between theoretical and experimental results. We have employed simple local empty-core pseudopotentials in this paper to calculate the effective pair potentials, because our main purpose of this paper is to investigate systematically the overall trend in the density dependence of the structure of expanded liquid alkali metals along the liquid–vapour coexistence curve. We have not, however, included Li in the present calculation, since it is well known that the non-local effect is essentially important for Li. In order to study the density dependence of the structure of expanded liquid Li, we need to use a more complicated non-local pseudopotential.

Acknowledgments

We are grateful to Professor F Hensel and Dr R Winter for sending us their experimental data. We also acknowledge Professor K Tamura and Dr S Hosokawa for useful discussions.

References

Bratkovsky A M, Vaks V G, Kravchuk S P and Trefilov A V 1982 *J. Phys. F: Met. Phys.* **12** 1293
Franz G 1980 *Thesis* University of Marburg
Franz G, Freyland W, Gläser W, Hensel F and Schneider E 1980 *J. Physique Coll.* **41** C8 194
Gillan M J 1979 *Mol. Phys.* **38** 1781
Gonzalez D J, Ng D A and Silbert M 1990 *J. Non-Cryst. Solids* **117, 118** 469
Hasegawa M, Hoshino K, Watabe M and Young W H 1990 *J. Non-Cryst. Solids* **117, 118** 300
Hoshino K, Matsuda N, Mori H and Watabe M 1990a *J. Non-Cryst. Solids* **117, 118** 44
Hoshino K, Matsuda N and Watabe M 1990b *J. Phys. Soc. Japan* **59** 2027
Hoshino K and Young W H 1986 *J. Phys. F: Met. Phys.* **16** 1659
Ichimaru S and Utsumi K 1981 *Phys. Rev.* B **24** 7385
Jüngst S, Knuth B and Hensel F 1985 *Phys. Rev. Lett.* **55** 2160
Kahl G and Hafner J 1984 *Phys. Rev.* A **29** 3310
Kahl G and Pastore G 1988 *Europhys. Lett.* **7** 37
Lado F, Foiles S M and Ashcroft N W 1983 *Phys. Rev.* A **28** 2374
McLaughlin I L and Young W H 1984 *J. Phys. F: Met. Phys.* **14** 1
Mori H, Hoshino K and Watabe M 1990 *J. Phys. Soc. Japan* **59** 3254
Mountain R D 1978 *J. Phys. F: Met. Phys.* **8** 1637
Pastore G and Kahl G 1987 *J. Phys. F: Met. Phys.* **17** L267
Rosenfeld Y and Ashcroft N W 1979 *Phys. Rev.* A **20** 1208
Shpil'rain E E, Yakimovich K A, Fomin V A, Skovorodjko S N and Mozgovoi A G 1985 *Handbook of Thermodynamic and Transport Properties of Alkali Metals* ed R W Ohse (Oxford: Blackwell) p 435
Tanaka M 1980 *J. Phys. F: Met. Phys.* **10** 2581
Waseda Y 1980 *The Structure of Non-crystalline Materials* (New York: McGraw Hill) p 254
Winter R, Hensel F, Bodensteiner T and Gläser W 1987 *Ber. Bunsenges. Phys. Chem.* **91** 1327

chromatized Cu K_α x-ray source as incident radiation. Temperatures regulated in the range 23 K to room temperature were obtained with a closed-circuit cryostat. The photographic study was completed by quantitative intensity measurements using a position-sensitive linear detector.

7.2. Results

Evidence for a low-temperature structural distortion is seen by comparison of the x-ray scattering patterns taken at about 30 K (figure 16(*a*)) and at about 65 K (figure 16(*b*)). Figure 16(*a*) shows supplementary Bragg reflections, with two types of intense satellite reflections present below 56.5 K:

(i) Incommensurate superlattice spots (identified with black arrows in figure 16(*a*)), which can be indexed by the reduced wavevector $\boldsymbol{q}_I = (1, \frac{1}{2}(1-\delta), 0)$ with respect to the main Bragg reflections of the high-temperature C-centred monoclinic lattice. The deviation from the commensurate wavevector $(1, \frac{1}{2}, 0)$ is very small, with δ equal to about 0.04, and this value does not vary significantly with temperature between 56.5 K and the lower limit of these experiments of 23 K.

(ii) Commensurate Bragg reflections (identified with white arrows in figure 16(*a*)), at the reduced wavevector $\boldsymbol{q}_B = (1, 0, 0)$. These break the C centring monoclinic symmetry of the high-temperature structure.

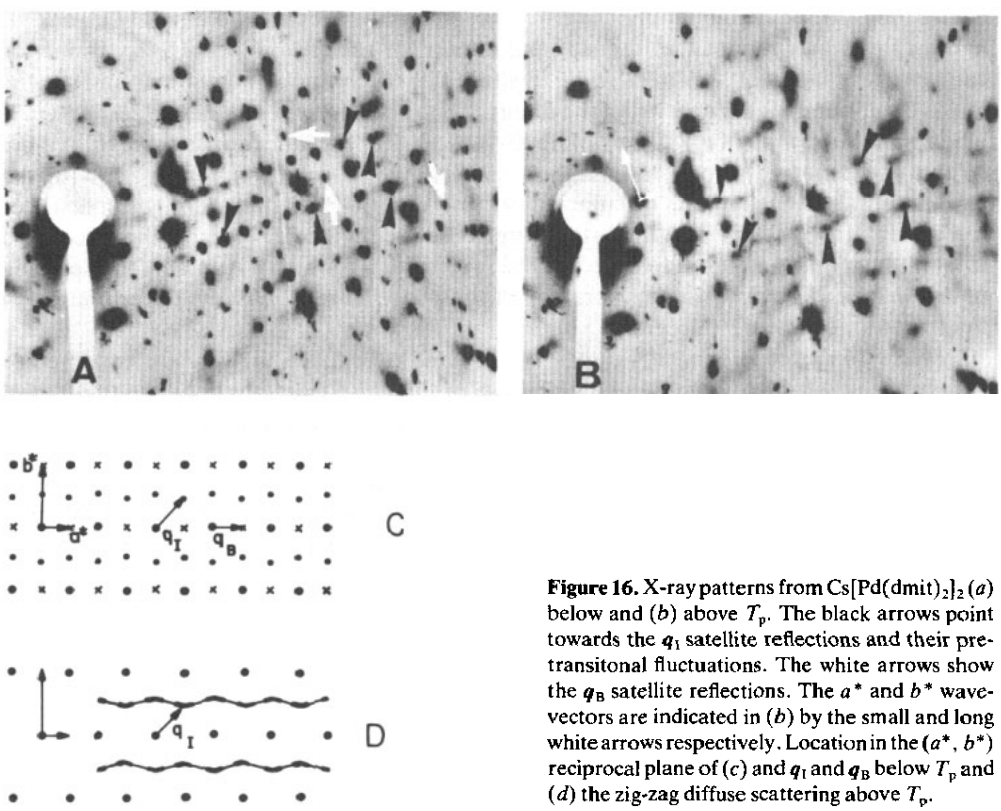

Figure 16. X-ray patterns from $Cs[Pd(dmit)_2]_2$ (*a*) below and (*b*) above T_p. The black arrows point towards the $\boldsymbol{q}_I$ satellite reflections and their pre-transitonal fluctuations. The white arrows show the $\boldsymbol{q}_B$ satellite reflections. The a^* and b^* wavevectors are indicated in (*b*) by the small and long white arrows respectively. Location in the (a^*, b^*) reciprocal plane of (*c*) and $\boldsymbol{q}_I$ and $\boldsymbol{q}_B$ below T_p and (*d*) the zig-zag diffuse scattering above T_p.